Received: 29 November 2022 | Revised: 9 February 2023 | Accepted: 13 February 2023

DOI: 10.1111/cas.15763

Cancer Science WILEY

ORIGINAL ARTICLE

Trigred motif 36 regulates neuroendocrine differentiation of prostate cancer via HK2 ubiquitination and GPx4 deficiency

Xusong Zhao[1] | Tianren Zhou[1] | Yuhao Wang[1] | Meiling Bao[2] | Chenbo Ni[1] | Lei Ding[1] | Shengjie Sun[3] | Huiyu Dong[1] | Jie Li[1] | Chao Liang[1]

[1]Department of Urology, The First Affiliated Hospital of Nanjing Medical University and Jiangsu Province Hospital, Nanjing, China

[2]Department of Pathology, The First Affiliated Hospital of Nanjing Medical University and Jiangsu Province Hospital, Nanjing, China

[3]Department of Urology, The Second Affiliated Hospital of Nanjing Medical University, Nanjing, China

Correspondence
Jie Li and Chao Liang, The First Affiliated Hospital of Nanjing Medical University and Jiangsu Province Hospital, 300 Guangzhou Road, Nanjing 210009, China.
Email: drc_lijie@126.com and cliang@njmu.edu.cn

Funding information
Jiangsu Provincial People's Hospital Clinical Capacity Enhancement Project, Grant/Award Number: JSPH-MC-2021-12; National Natural Science Foundation of China, Grant/Award Number: 82002718; Natural Science Foundation of Jiangsu Province, Grant/Award Number: BK20191077

Abstract

Neuroendocrine prostate cancer (NEPC), the most lethal subtype of castration-resistant prostate cancer (PCa), may evolve from the neuroendocrine differentiation (NED) of PCa cells. However, the molecular mechanism that triggers NED is unknown. Trigred motif 36 (TRIM36), a member of the TRIM protein family, exhibits oncogenic or anti-oncogenic roles in various cancers. We have previously reported that TRIM36 is highly expressed to inhibit the invasion and proliferation of PCa. In the present study, we first found that TRIM36 was lowly expressed in NEPC and its overexpression suppressed the NED of PCa. Next, based on proteomic analysis, we found that TRIM36 inhibited the glycolysis pathway through suppressing hexokinase 2 (HK2), a crucial glycolytic enzyme catalyzing the conversion of glucose to glucose-6-phosphate. TRIM36 specifically bound to HK2 through lysine 48 (lys48)-mediated ubiquitination of HK2. Moreover, TRIM36-mediated ubiquitination degradation of HK2 downregulated the level of glutathione peroxidase 4 (GPx4), a process that contributed to ferroptosis. In conclusion, TRIM36 can inhibit glycolysis via lys48-mediated HK2 ubiquitination to reduce GPX4 expression and activate ferroptosis, thereby inhibiting the NED in PCa. Targeting TRIM36 might be a promising approach to retard NED and treat NEPC.

KEYWORDS
HK2, NED, PCa, TRIM36, ubiquitination

1 | INTRODUCTION

PCa is an androgen-dependent disease and androgen deprivation therapy (ADT) is considered the most effective regimen to treat metastatic disease. Studies have shown that the occurrence of NEPC is closely related to long-term ADT. ADT promotes the transformation from PCa to NEPC, a possible mechanism driving drug resistance.[1,2] Despite treatment with new anti-androgen therapeutics, advanced prostate cancer may still progress to NEPC.[3,4] NEPC includes a large nucleocytoplasmic ratio, deep staining, and close distances between nuclei. Immunohistochemical staining shows negative androgen receptor (AR) and positive neuroendocrine markers which usually bring death within 1–2 years after diagnosis.[5,6] With the wide use of new androgen receptor-targeted therapy, the incidence of NEPC is expected to increase, making it urgent to delve into the pathogenesis of NEPC before designing new effective treatments.

Xusong Zhao, Tianren Zhou, and Yuhao Wang contributed equally to this article.

TRIM36, a member of the TRIM family, was preliminarily identified in the testis of adult mice. Its transcripts are highly expressed in the testis of mice, but almost not in other organs.[7] Balint et al. identified TRIM36 as an androgen-responsive gene from the tumor suppressor gene region at chromosome 5q22. 3.[8,9] Naoki et al. demonstrated that TRIM36 plays a tumor-suppressive role in PCa.[10] It was theorized that tumor occurence possibly disabled tumor cells ability for aerobic respiration.[11] To ensure self-survival as well as to meet the increasing demand for biosynthetic precursors, tumor cells activate other energy production pathways and rewire their glucose metabolism to aerobic glycolysis. However, many of these energy metabolic aberrations converge on ferroptosis and profoundly affect its initiation and execution.[13] All these put forward conjectures and hypotheses for the role of TRIM36 in NEPC. We previously created tissue micro arrays (TMAs) (patients and tissue microarrays) of 95 prostate cancer tissues (obtained from patients who were treated by radical prostatectomy between 2008 and 2011 at the First Affiliated Hospital of Nanjing Medical University) and follow-up experiments have confirmed that TRIM36 can inhibit the invasion and proliferation of PCa through the MAPK ERK kinase (MAPK/ERK) phosphorylation pathway, and enhance the sensitivity of PCa cells to enzalutamide.[14] However, no study has described the roles of TRIM36 in NEPC.

In this study, we found that TRIM36 as a novel androgen-responsive gene regulated tumor plasticity in NEPC by suppressing glutathione GPx4 expression in an HK2-ubiquitination manner. The underlying mechanism is that TRIM36 was upregulated during ADT, which enhanced the modification of HK2 with lys48-linked ubiquitination to inhibit glycolysis. Moreover, HK2 depletion decreased the expression of GPx4, which finally facilitated the death of ferroptosis. Suppression of glycolysis and activation of ferroptosis regulated the NED of PCa. Those effects were reversed by sh-TRIM36. Thus, our study suggests that TRIM36 reduction of GPx4 expression via HK2 ubiquitination is an important mechanism in regulating NEPC.

2 | MATERIALS AND METHODS

2.1 | Antibodies and reagents

Unless otherwise indicated, all antibodies were used at a dilution of 1:1000. Antibodies and reagents are detailed in Table S1.

2.2 | Cell culture

The LNCaP, LNCap95, C4-2, DU145, and PC-3 human prostatic cancer cell lines were obtained from the Cell Bank Type Culture Collection. The PC-3 cells were cultured in an F-12K Nutrient Mixture (Gibco), and the LNCaP, LNCap95, C4-2, and DU145 cells were cultured in RPMI-1640 (Gibco). All media were supplemented with 10% fetal bovine serum (Gibco) and cells were maintained in a humidified atmosphere containing 5% CO_2 at 37°C.

2.3 | Cell transfection

Two lentiviral vectors with TRIM36 shRNA and one that overexpressed TRIM36 were constructed by Genechem. A lentiviral vector with negative control (NC) shRNA was used as a negative control for the TRIM36 knockdown and TRIM36 overexpression. pCMV-HA-ubiquitin (K48R), pCMV-HA-ubiquitin (K63R), and pCMV-HA-ubiquitin (wt) were designed and synthesized by the Haijihaoge Biology Company. The small interfering RNAs of HK2 were designed and synthesized by PROTEINBIO Biology Company. Lipofectamine™ 3000 transfection reagent (ThermoFisher) was used for transfection.

2.4 | RNA isolation and quantificational rt-PCR (qRT-PCR)

Trizol (Invitrogen) was used for RNA extraction from LNCaP and PC-3 cell lines according to the manufacturer's instructions. Mirna was reverse-transcribed into cDNA using MiR-XTM miRNA First-Strand Synthesis (Takara). Total RNA was reversed-transcribed into cDNA using PrimeScript RT Master Mix (Takara). A standard SYBR Green PCR kit (Takara) was used to perform qRT-PCR. The primer sequences used for quantitative RT-PCR are detailed in Table S2. Fold changes in gene expression were calculated after normalization to their corresponding beta-actin mRNA levels.

2.5 | Western blotting

Proteins were isolated from cells with RIPA lysis buffer (Sigma-Aldrich). Protein content was measured with a Bicinchoninic acid (BCA) protein assay kit (Thermo Fisher Scientific). Using SDS-PAGE protein lysates were separated and then transferred to PVDF membranes. After blocking the membranes with TBS+Tween (TBST) including 5% milk, the primary antibodies were incubated overnight at 4°C then incubated with horseradish peroxidase-conjugated secondary antibodies and visualized using an enhanced chemiluminescence kit (Santa Cruz). Protein bands were quantified with Quantity One software (Bio-Rad) using GAPDH as an internal reference.

FIGURE 1 TRIM36 is downregulated in NEPC. (A) Expression of TRIM36 mRNA in patients with PCa, CRPC ($n = 31$), and CRPC-NE ($n = 15$). Values are expressed as the mean ± SEM. $^{*}P < 0.05$. (B) Expression of TRIM36 in patients with different Gleason scores in TCGA database. Columns, mean; error bars, standard deviation. $^{*}P < 0.05$; $^{**}P < 0.01$. (C) Correlation between TRIM36, AR, and KLK3 expression in TCGA database. RAR = 0. 26 , RKLK3 = 0. 31, $P < 0.05$. (D) Correlation between TRIM36, CHGA, and ENO_2 expression in TCGA database. RCHGA = −0.25, RENO2 = −0. 33, $P < 0.05$. (E) IHC was performed on 20 PCa patients with TRIM36, KLK3, AR, ENO2, and CHGA antibodies. Tissue was grouped into primary tumors ($n = 10$) and NEPC ($n = 10$), with two representative images from matched tissue from each group shown. Scale bar: 50 μm. (F) IHC scores of TRIM36, KLK3, AR, ENO2, and CHGA were plotted. $^{*}P < 0.05$, $^{**}P < 0.01$, $^{***}P < 0.001$

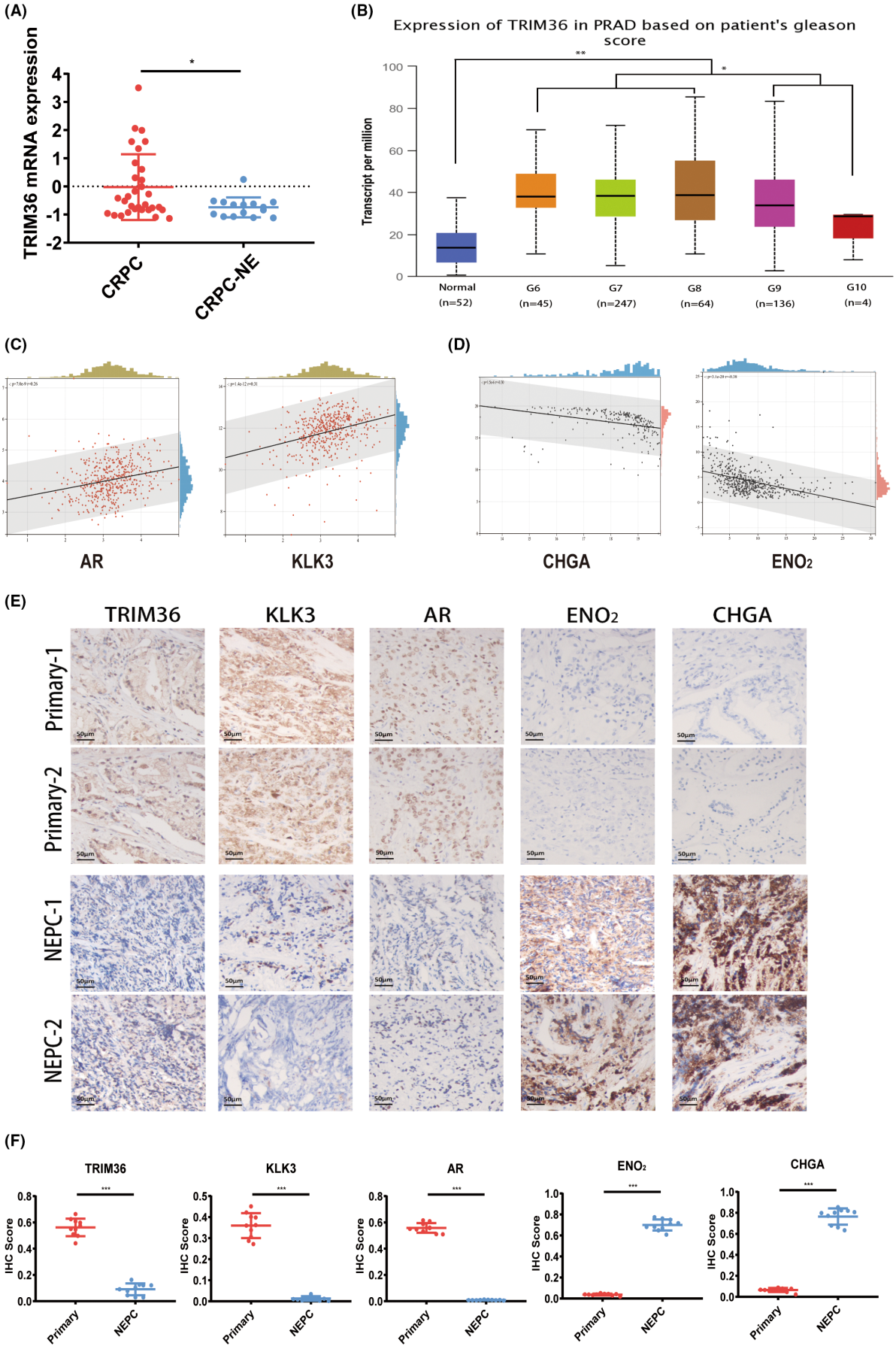
(A)
TRIM36 mRNA expression
CRPC
CRPC-NE
(B)
Expression of TRIM36 in PRAD based on patient's gleason score
Transcript per million
Normal (n=52)
G6 (n=45)
G7 (n=247)
G8 (n=64)
G9 (n=136)
G10 (n=4)
(C)
AR
KLK3
(D)
CHGA
ENO2
(E)
TRIM36
KLK3
AR
ENO2
CHGA
Primary-1
Primary-2
NEPC-1
NEPC-2
(F)
TRIM36
KLK3
AR
ENO2
CHGA
IHC Score
Primary
NEPC

2.6 | Immunoprecipitation (IP) and co-immunoprecipitation (Co-IP)

Cell extract was supplemented with a mixture of protease inhibitors and phosphatase inhibitors. The mixture (kgp603 and kgp602; Jiangsu Kaiji Biotechnology Co., Ltd.) was produced by the cracking buffer (p0013b; Shanghai Biyuntian Biotechnology Co., Ltd.). For IP and Co-IP, an immunoprecipitation kit (abs955; Shanghai Aibixin Biotechnology Co., Ltd.) was used. The protein was denatured by SDS sample buffer and boiled at 100°C for 15 min then separated by SDS-PAGE. Western blotting analysis.

2.7 | Determination of glucose consumption and lactate production

The glucose oxidase method was used to determine the optical density (OD) value obtained by the reagent kit (e1010; Beijing Pulley Gene Technology Co., Ltd.) according to instructions. The standard curve was plotted and the glucose concentration of the sample was measured. A lactic acid assay kit (a019-2-1; Nanjing Jiancheng Biotechnology Co., Ltd.) was used to determine the OD value. Sample lactic acid content = (measured OD value blank OD value)/(standard OD value blank OD value) × standard concentration × sample dilution ratio.

2.8 | Mass spectrometry

The immunoblotting was terminated after the electrophoresis step. The adhesive was removed and cut according to the markers. The adhesive strip was removed with double-distilled water. The configured Coomassie brilliant blue R250 was put into a clean incubation box, followed by the addition of the adhesive strip. Then the box was placed on the shaking table for dyeing at room temperature for 1 h or overnight. After dyeing, the dyeing solution was poured out carefully and the strip was retained. The decolorizing solution was then added and the mixture was further eluted on the shaking table. The eluent was replenished at 0.5, 2, 8, and 20 h (the elution duration and times were determined by the protein color and strip color). Elution was stopped when the blank of the strip became transparent and the protein dyeing had not been eluted. The glue was cut for enzymolysis. First, the disulfide bond was opened and the sulfhydryl group was closed. Trypsin enzymolysis was allowed to open the C-terminal peptide bond of arginine/lysine, and finally the salt ions of the peptide segment were removed. Liquid chromatography-tandem mass spectrometry was performed after enzymatic hydrolysis. After obtaining the original mass spectrometry data, the matched protein database was retrieved, and then the sample quality was assessed according to the deviation of mass spectrometry detection and enzyme digestion efficiency. Finally, the data were analyzed to screen the differential proteins.

2.9 | Xenograft

Mouse experiments were approved by the animal research ethics committee of Nanjing Medical University. For flank implantation, 5-week-old male nude mice were randomly divided into two groups, with five mice in each group. Stable cells LNCaP-NC, LNCaP-ST, PC3-NC, and PC3-OV (5×10^6) suspended in 150 μL of PBS were injected subcutaneously into the flank of each mouse. After 2–3 weeks, the tumor was removed and the tissue samples were fixed and paraffin-embedded.

2.10 | Immunohistochemistry

Xenograft tumors and patient tissue (see Table S1 for patient information) were fixed in 4% paraformaldehyde overnight, embedded in paraffin, sectioned, and stained with primary antibodies against the following proteins or epitope tags: TRIM36 (qc13477), HK2 (c64g5), AR (ab198394), kallikrein-3 (KLK3/PSA)(ab76113), chromogranin A (CHGA)(AB283265), synaptophysin (SYP)(d40c4), aurora-kinase-A (AURKA)(ab13824) and enolase 2 (ENO2/NSE)(ab53025). The visual fields were randomly selected from each sample, and the OD value of the sample dyeing intensity was scored through image J software. The OD value conformed to Lambert Beer's law and its mathematical expression is $A = \log(1/T) = Kbc$, where A is absorbance, T is transmissivity, K is molar absorption coefficient, c is the concentration of light-absorbing material (mol/L), and b is the thickness of absorption layer (cm). The pathological evaluation of these tumors was performed independently by three pathologists.

2.11 | Bioinformatics analysis methods

Data from 496 PCa cases were collected from The Cancer Genome Atlas (TCGA) database. The patients' RNA sequencing (SEQ)

FIGURE 2 TRIM36 inhibited the NED in PCa cell lines. (A) TRIM36 mRNA and protein levels in LNCaP, LNCaP95, and PC3 cell lines. Columns, mean; error bars, standard deviation. $^*P < 0.05$. (B) Construction of TRIM36 knockdown/overexpression cell lines. qRT-PCR and Western blotting were used to detect TRIM36 mRNA and protein expression. Knockdown/overexpression efficiency. Columns, mean; error bars, standard deviation. $^*P < 0.05$, $^{**}P < 0.01$, $^{***}P < 0.001$. (C) Cell morphologies of LNCaP-NC, LNCaP-ST, PC3-NC, and PC3-OV cells. Scale bar: 50 μm. (D) mRNA and protein expression of NED-related markers in LNCaP-ST and control group, PC3-OV and control group. Columns, mean; error bars, standard deviation. $^*P < 0.05$

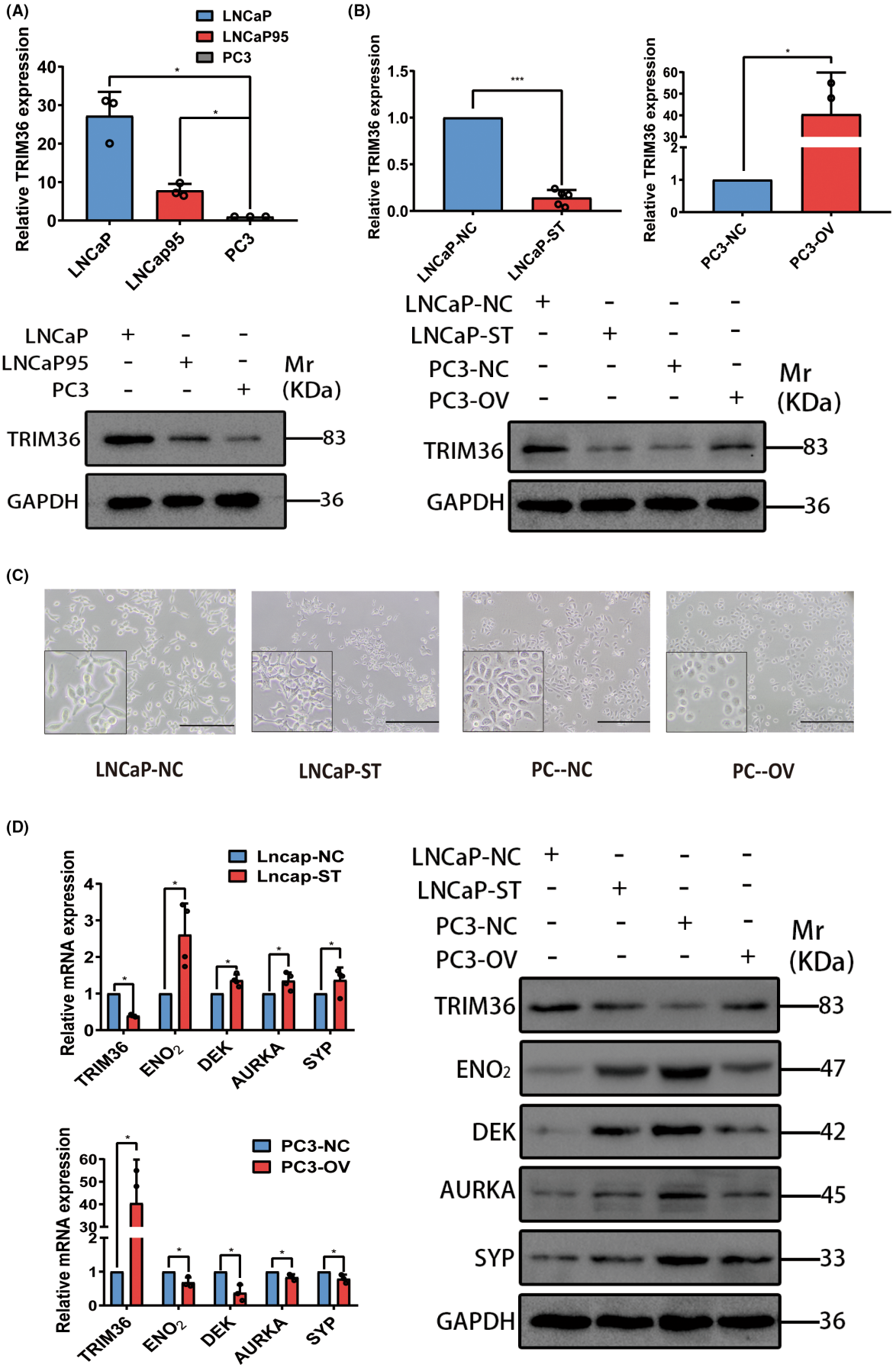
(A)
LNCaP
LNCaP95
PC3
Relative TRIM36 expression
LNCaP
LNCap95
PC3
LNCaP + - -
LNCaP95 - + -
PC3 - - +
Mr (KDa)
TRIM36
GAPDH
83
36
(B)
Relative TRIM36 expression
LNCaP-NC
LNCaP-ST
PC3-NC
PC3-OV
LNCaP-NC + - - -
LNCaP-ST - + - -
PC3-NC - - + -
PC3-OV - - - +
Mr (KDa)
TRIM36
GAPDH
83
36
(C)
LNCaP-NC
LNCaP-ST
PC--NC
PC--OV
(D)
Lncap-NC
Lncap-ST
Relative mRNA expression
TRIM36
ENO2
DEK
AURKA
SYP
PC3-NC
PC3-OV
LNCaP-NC + - - -
LNCaP-ST - + - -
PC3-NC - - + -
PC3-OV - - - +
Mr (KDa)
TRIM36
ENO2
DEK
AURKA
SYP
GAPDH
83
47
42
45
33
36

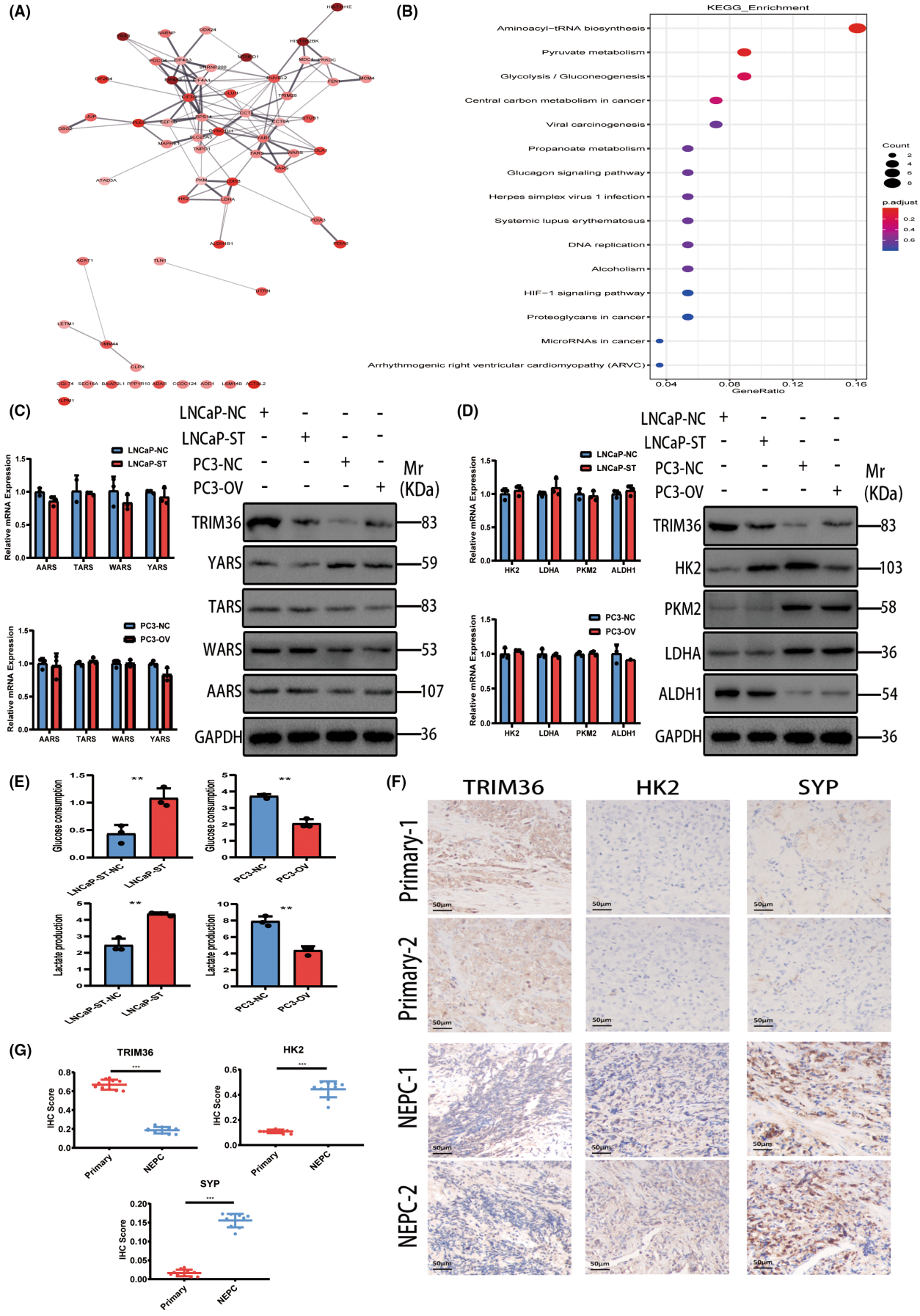
(A)
(B)
KEGG_Enrichment
Aminoacyl−tRNA biosynthesis
Pyruvate metabolism
Glycolysis / Gluconeogenesis
Central carbon metabolism in cancer
Viral carcinogenesis
Propanoate metabolism
Glucagon signaling pathway
Herpes simplex virus 1 infection
Systemic lupus erythematosus
DNA replication
Alcoholism
HIF−1 signaling pathway
Proteoglycans in cancer
MicroRNAs in cancer
Arrhythmogenic right ventricular cardiomyopathy (ARVC)
GeneRatio
Count
p.adjust
(C)
LNCaP-NC
LNCaP-ST
PC3-NC
PC3-OV
Mr (KDa)
Relative mRNA Expression
AARS
TARS
WARS
YARS
TRIM36
YARS
TARS
WARS
AARS
GAPDH
83
59
83
53
107
36
(D)
HK2
LDHA
PKM2
ALDH1
TRIM36
HK2
PKM2
LDHA
ALDH1
GAPDH
83
103
58
36
54
36
(E)
Glucose consumption
Lactate production
LNCaP-ST-NC
LNCaP-ST
PC3-NC
PC3-OV
(F)
TRIM36
HK2
SYP
Primary-1
Primary-2
NEPC-1
NEPC-2
50μm
(G)
TRIM36
HK2
SYP
IHC Score
Primary
NEPC

FIGURE 3 Identification of TRIM36 target genes in PCa. (A, B) KEGG enrichment analysis results. (C) qRT-PCR and Western blotting were used to detect the mRNA and protein expression of genes related to the aminoacyl tRNA biosynthesis pathway in PCa cells after interference and overexpression of TRIM36. Columns, mean; error bars, standard deviation. (D) The mRNA and protein expression levels of glycolysis-related genes in LNCaP-ST, PC3-OV, and control cells. Columns, mean; error bars, standard deviation. (E) Comparison of glucose consumption and lactic acid production between LNCaP-ST and control cells, PC3-OV and control cells. Columns, mean; error bars, standard deviation. $^{*}P<0.05$, $^{**}P<0.01$. (F) IHC was performed on 20 PCa patients with TRIM36, HK2, and SYP antibodies. Tissue was grouped into primary tumors ($n=10$) and NEPC ($n=10$), with two representative images from matched tissue from each group shown. Scale bar: 50 μm. (G) IHC scores of TRIM36, HK2, and SYP were plotted. Values are expressed as the mean ± SEM. $^{*}P<0.05$, $^{**}P<0.01$, $^{***}P<0.001$

expression matrices and supporting clinical information were sorted into a data format that can be recognized by R software. The two-gene correlation map was realized by the R software package ggstatsplot. Spearman's correlation analysis was used to describe the correlation between quantitative variables without normal distribution. *P* values less than 0.05 were considered statistically significant.

2.12 | Immunofluorescence staining

Cells were seeded on slides at an appropriate density, fixed with paraformaldehyde, treated with 0. 3% Triton X-100 for permeabilization, and stained with antibodies, including anti-TRIM36 (1:200), anti-HK2 (1:200), and 4',6-diamidino-2-phenylindole (DAPI). The expression of target proteins (red or green) and DAPI (blue) were examined by fluorescence microscopy.

2.13 | Data analysis

All experiments were performed at least in triplicate. Statistics were standardized as described. In brief, statistical analysis was performed using Microsoft Excel and GraphPad Prism software. For paired *t*-tests, all experimental groups were compared with their respective groups. Student's *t*-test was used to determine the statistical difference between the two groups. Significant differences ($^{*}P\le0.05$, $^{**}P\le0.01$, $^{***}P\le0.001$) are indicated in the figures with asterisks.

3 | RESULTS

3.1 | TRIM36 expression is downregulated in NEPC

TRIM36 overexpression has been observed in PCa tissues[8] and this observation was confirmed in our previous research. Analyzing the sequencing results of Beltran et al.,[15] we found that the expression of TRIM36 in Castration-Resistant neuroendocrine prostate cancer (CRPC-NE) tissue (a subset of resistant tumors shows small-cell carcinoma or neuroendocrine features on metastatic biopsy) is significantly lower than that in Castration-Resistant Prostate Cancer (CRPC) tissue (Figure 1A). We then detected that TRIM36 was negatively correlated with the malignancy of PCa based on TCGA database (Figure 1B,C). Further applying Immunohistochemistry (IHC) to tissue from the department of pathology (The First Affiliated Hospital of Nanjing Medical University, Nanjing, China) containing 20 primary tumors and 20 NEPC tissues showed that NED markers CHGA and ENO2/NSE are highly expressed with TRIM36, KLK3/PSA, and AR decreasing in NEPC tissues (Figure 1E,F). This is consistent with the above bioinformatics analysis results, and we suspect that TRIM36 inhibited the NED of PCa.

3.2 | TRIM36 inhibited the NED in PCa cell lines

We verified the expression of TRIM36 in PCa cell lines. As shown in Figure 2A, TRIM36 expression decreased in PCa cell lines LNCaP (androgen-dependent), LNCaP95 (androgen-independent), and PC3 (neuroendocrine differentiation), indicating that TRIM36 decreased with the progression of PCa cells. To screen suitable cell lines, we verified the expression of TRIM36 and the NED-related gene ENO2 in several commonly used PCa cell lines. Among LNCaP, C4-2, DU145, and PC3 cells, the highest expression of TRIM36 was in LNCaP cells and the lowest expression of TRIM36 was in PC3 cells, which is contrary to the ENO2 expression trends (Figure S1). Next, we constructed LNCaP-ST and C4-2-ST with stable underexpression of TRIM36, and DU145-OV and PC3-OV with stable overexpression of TRIM36 (Figure 2B). Compared with those in the control group, the cell morphology of LNCaP-ST changed, the nuclear volume increased, the number of dendrites increased, the PC3-OV cells became smaller and almost circular, and their dendrites decreased significantly (Figure 2C). This phenotype difference was also consistent with the changes in cellular NED. However, no morphological changes were seen in C4-2-ST and DU145-OV cells (Figure S2A,B). Further verification found that although C4-2-ST and DU145-OV cells had no morphological changes, Western blotting-results showed that the change of -TRIM36 expression still affected the protein expression of NED-related markers (Figure S2C). Finally, we selected PCa cell lines LNCaP and PC3 cells line for further research. We detected the expression of NED markers ENO2, DEK oncogene(DEK), AURKA, and SYP in LNCaP-ST and PC3-OV cells by qRT-PCR and Western blotting. Compared with that in the control group, the expression of NED markers was elevated, while the results were the opposite in PC3-OV cells (Figure 2D). We therefore

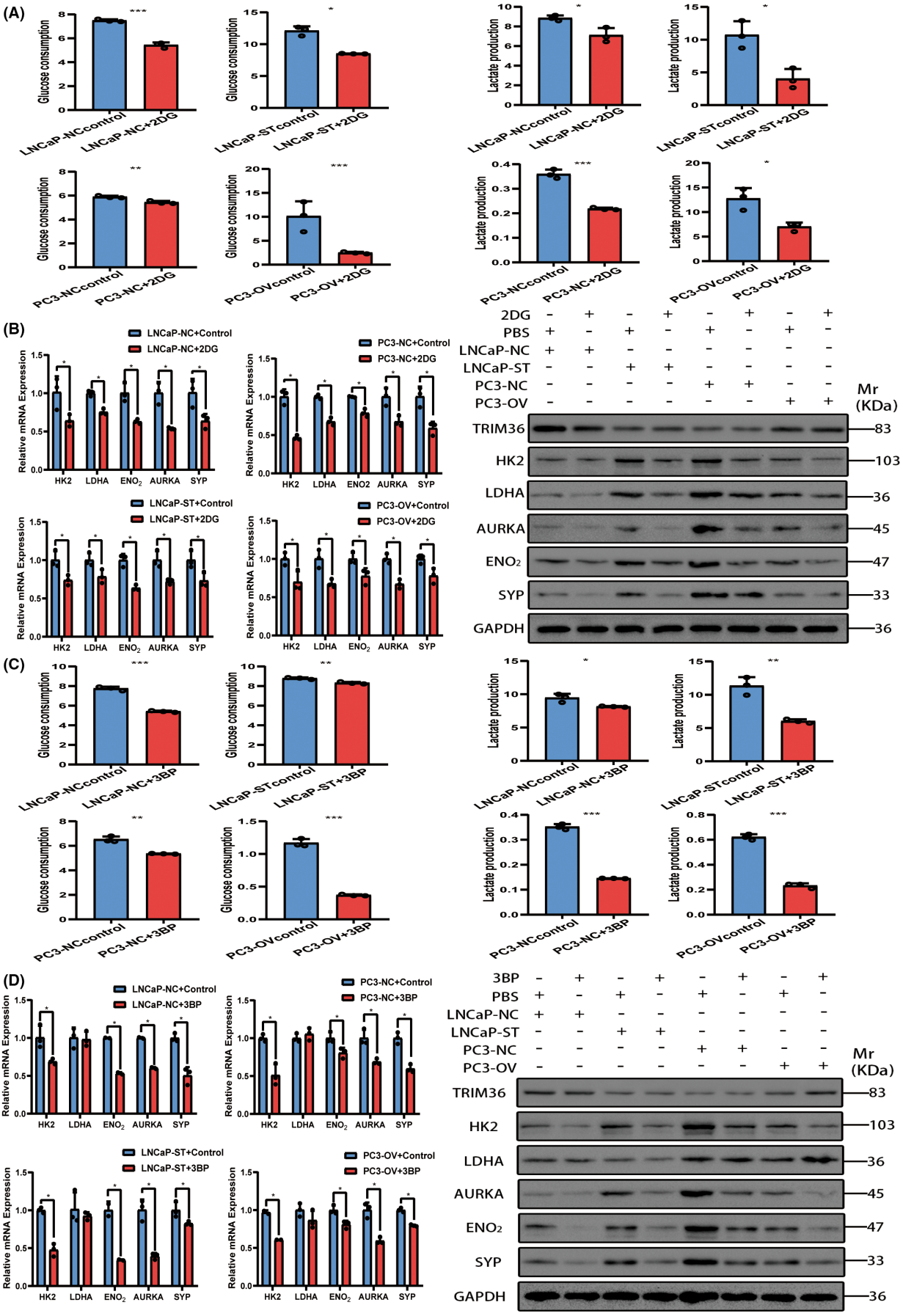
(A)
Glucose consumption
Lactate production
LNCaP-NCcontrol
LNCaP-NC+2DG
LNCaP-STcontrol
LNCaP-ST+2DG
PC3-NCcontrol
PC3-NC+2DG
PC3-OVcontrol
PC3-OV+2DG
(B)
LNCaP-NC+Control
LNCaP-NC+2DG
PC3-NC+Control
PC3-NC+2DG
LNCaP-ST+Control
LNCaP-ST+2DG
PC3-OV+Control
PC3-OV+2DG
Relative mRNA Expression
HK2
LDHA
ENO2
AURKA
SYP
2DG
PBS
LNCaP-NC
LNCaP-ST
PC3-NC
PC3-OV
Mr (KDa)
TRIM36
HK2
LDHA
AURKA
ENO2
SYP
GAPDH
83
103
36
45
47
33
36
(C)
LNCaP-NC+3BP
LNCaP-ST+3BP
PC3-NC+3BP
PC3-OV+3BP
(D)
3BP

FIGURE 4 Pharmacological inhibition of HK2 blocked NED of PCa cells. (A) Glucose consumption and lactate production in LNCaP-NC, LNCaP-ST, PC3-NC, and PC3-OV cells treated with glycolysis-inhibitor 2DG. Columns, mean; error bars, standard deviation. $^{*}P<0.05$, $^{**}P<0.01$, $^{***}P<0.001$. (B) qRT PCR and Western blotting were used to detect the expression of glycolysis-related genes and NED-related genes in PCa cells before and after 2DG treatment. Columns, mean; error bars, standard deviation. $^{*}P<0.05$. (C) Glucose consumption and lactate production in LNCaP-NC, LNCaP-ST, PC3-NC, and PC3-OV cells treated with HK2 inhibitor 3BP. Columns, mean; error bars, standard deviation. $^{*}P<0.05$, $^{**}P<0.01$, $^{***}P<0.001$. (D) The expression of glycolysis-related genes and NED-related genes in PCa cells before and after 3BP treatment was detected by qRT-PCR and Western blotting. Columns, mean; error bars, standard deviation. $^{*}P<0.05$

speculated that underexpression of TRIM36 promoted and overexpression of TRIM36 inhibited the NED of PCa cells.

3.3 | Identification of TRIM36 target genes in PCa

To explore the regulatory mechanism of TRIM36 in NED, we detected the proteins interacting with TRIM36 and downstream pathways. Through immunocoprecipitation, the TRIM36 antibody helped us obtain the target protein from the protein mixture. The components of these proteins were confirmed by mass spectrometry. As shown in the Kyoto Encyclopedia of Genes and Genomes (KEGG) pathway enrichment analysis, TRIM36 was involved in three possible pathways: the aminoacyl tRNA biosynthesis pathway, the pyruvate metabolism pathway, and the glycolysis/gluconeogenesis pathway (Figure 3A,B). By detecting the expression of markers alanyl-tRNA synthetase (AARS), Aminoacyl-tRNA synthases (TARS), tryptophanyl-tRNA synthetase (WARS), and tyrosyl-tRNA synthetase (YARS) related to aminoacyl tRNA biosynthesis, the results showed that TRIM36 had no significant correlation with aminoacyl tRNA biosynthesis pathway (Figure 3C). The second and third pathways were then analyzed. Because the pyruvate metabolism pathway is a downstream pathway of glycolysis or gluconeogenesis, we first selected the glycolysis pathway-related genes HK2, pyruvate kinase M2 (PKM2), lactate dehydrogenase A (LDHA), and acetaldehyde dehydrogenase 1 (ALDH1) for detection. We found the expression of HK2 decreased as the expression of TRIM36 increased at the protein level (Figure 3D). We detected the glucose consumption and lactate production of LNCaP-ST and PC3-OV cells. It was found that underexpression of TRIM36 increased glucose consumption and lactate production, and overexpression of TRIM36 decreased glucose consumption and lactate production (Figure 3E). IHC scores also showed that HK2 and SYP have low expression in primary tumors and are highly expressed in NEPC tissues ($P<0.001$) (Figure 3F,G). This suggests that TRIM36 retards the NED of PCa cells by inhibiting glycolysis.

3.4 | Pharmacological inhibition of HK2 blocked NED of PCa cells

Considering the close relationship between glycolysis and NED, we inhibited the glycolysis pathway with 2-deoxy-D-glucose (2DG) treatment (Figure 4A). The inhibition of the glycolysis pathway result in NED-related genes silence (Figure 4B). Further selecting HK2 inhibitor 3-bromopyruvate (3BP) to treat cells (Figure 4C), we found that inhibition of HK2 led to inhibition of the glycolysis pathway and then inhibition of the NED of PCa cells (Figure 4D), therefore TRIM36 inhibited the NED of PCa cells by inhibiting the expression of glycolysis-related protein HK2.

3.5 | TRIM36 ubiquitinated HK2 and inhibited the NED of PCa cells

Because of the protein expression level of TRIM36 was negatively correlated with that of HK2, we exploited immunofluorescence staining to observe TRIM36 and HK2 expression in PCa cells. The observation results are consistent with our conclusions and TRIM36 co localized with the HK2 which prompted TRIM36 may specifically bound to HK2 (Figure 5A). To verify the interaction between TRIM36 and HK2, we used the antibody of TRIM36 for the Co-IP experiment and detected HK2 in the immune complex. At the same time, the Co-IP experiment was repeated with the antibody of HK2, and TRIM36 was also detected in the immune complex (Figure 5B). This proved to be an interaction between endogenous TRIM36 and endogenous HK2, and TRIM36 can bind specifically to HK2. Prompted by the above findings, we analyzed the molecular events involved in this interaction. The most prevalent autophagy-targeting signal in mammals is the ubiquitination of cargo.[16,17] Whereas, TRIM36 can function as an E3 ubiquitin ligase. This suggests whether ubiquitination occured between TRIM36 and HK2. To determine whether TRIM36-HK2 interaction is related to ubiquitination, we repeated the IP experiment. Compared with the control cells, TRIM36 knockdown showed significantly lower HK2 ubiquitination levels, while TRIM36 overexpression showed higher HK2 ubiquitination levels (Figure 5C). We then evaluated the ubiquitination of HK2 by TRIM36 and the degradation of HK2 mediated by ubiquitin protease using the proteasome inhibitor MG132. It was found that the ubiquitin protease was suppressed as MG132 treated the cells for a longer period of time, such that the HK2 labeled with the ubiquitin protein was not degraded by the ubiquitin enzyme and accumulated. This indicates that TRIM36 can tag and degrade HK2 by ubiquitination (Figure 5D). Next, we explored which ubiquitination chain TRIM36 used to ubiquitinate HK2. K48R ubiquitin mutant (unable to form K48-linked chains) impaired HK2 polyubiquitination, whereas the K63R mutant (unable to form K63-linked chains) did not (Figure 5E). Our results were verified through an IP test on PCa cells. It was found that the expression of K48-linked ubiquitin protein was inhibited because of the TRIM36 underexpression and was enhanced

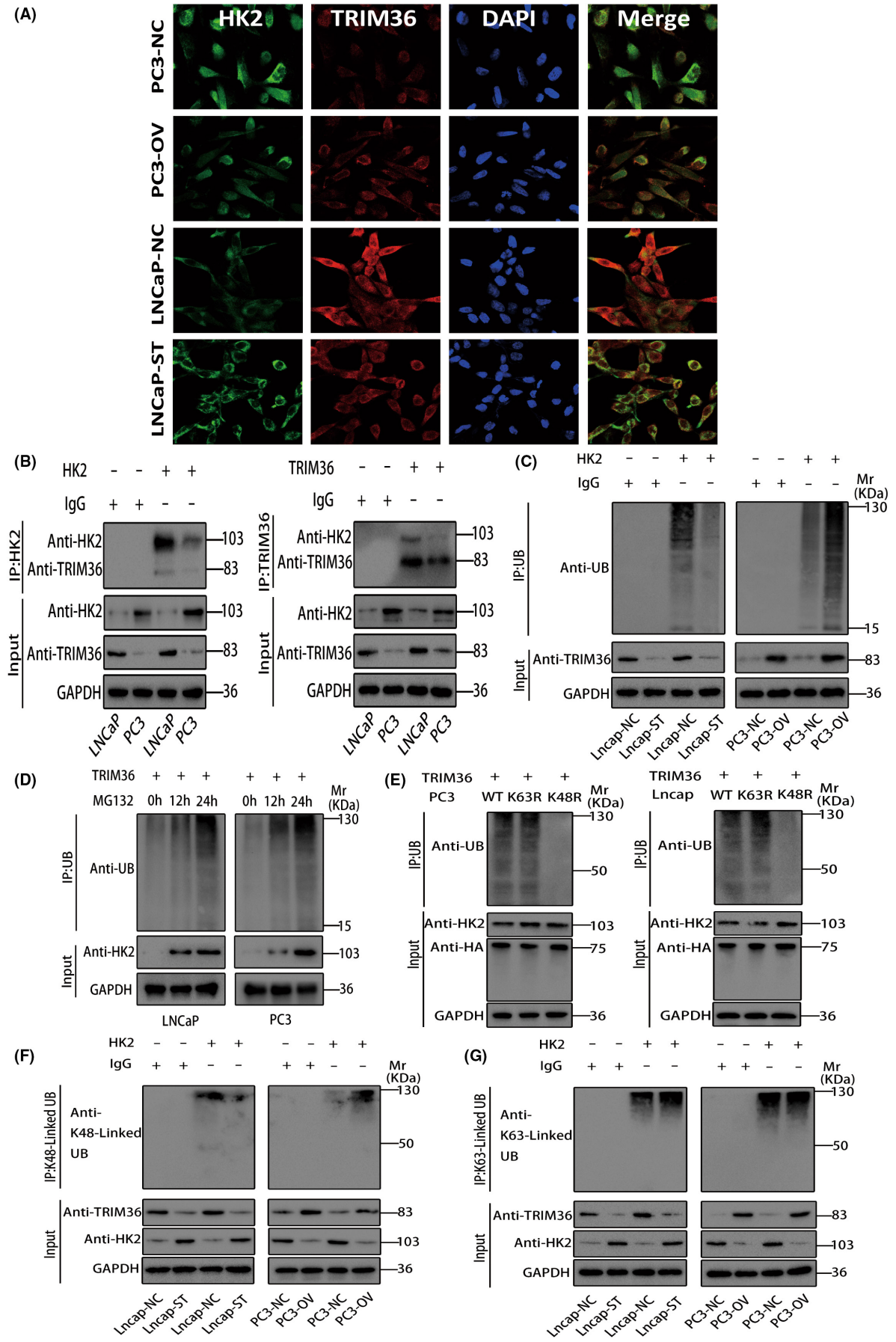
(A)
HK2
TRIM36
DAPI
Merge
PC3-NC
PC3-OV
LNCaP-NC
LNCaP-ST
(B)
HK2
IgG
IP:HK2
Anti-HK2
Anti-TRIM36
Input
GAPDH
103
83
36
LNCaP
PC3
TRIM36
IP:TRIM36
(C)
IP:UB
Anti-UB
Mr (KDa)
130
15
Lncap-NC
Lncap-ST
PC3-NC
PC3-OV
(D)
MG132
0h 12h 24h
(E)
PC3
Lncap
WT K63R K48R
Anti-HA
75
50
(F)
IP:K48-Linked UB
Anti-K48-Linked UB
(G)
IP:K63-Linked UB
Anti-K63-Linked UB

FIGURE 5 TRIM36 ubiquitinated HK2 and inhibited the NED of PCa cells. (A) Immunostaining showing the HK2 (green) and TRIM36 (red) in the LNCaP-NC, LNCaP-ST, PC3-NC, and PC3-OV cells. (B) CO-IP experiments were carried out based on the lysates of LNCaP and PC3 cells with TRIM36 and HK2 antibodies to analyze TRIM36-HK2 interaction. (C) Cell lysates were immunoprecipitated with antibodies against HK2 to detect the ubiquitination levels in LNCaP-NC, LNCaP-ST, PC3-NC, and PC3-OV cells. (D) LNCaP and PC3 cells were treated with MG132 for 0, 12, and 24 h, respectively, and their cell lysates were co-immunoprecipitated with anti-TRIM36 antibodies to detect whether TRIM36 could ubiquitin degrade its substrate protein HK2. (E) LNCaP and PC3 cells were transfected with wild-type, lys48 mutant, and lys63 mutant plasmids. The cell lysates were co-immunoprecipitated with TRIM36 antibody to detect their ubiquitination levels. (F) LNCaP-NC, LNCaP-ST, PC3-NC, and PC3-OV cells were immunoprecipitated with HK2 antibody, and the expression of K48-linked ubiquitin in the immune complex was detected. (G) The expression of K63-linked ubiquitin in cell lysates of LNCaP-NC, LNCaP-ST, PC3-NC, and PC3-OV cells was detected by IP test with HK2 antibody

by TRIM36 overexpression (Figure 5F). In addition, K63-linked ubiquitin did not change with TRIM36 transformation (Figure 5G). We therefore determined that TRIM36 could ubiquitinate HK2 through the lys48 chain to inhibit the NED of PCa cells.

3.6 | TRIM36 regulated NED of PCa cells via HK2-GPX4-ferroptosis

To examine how TRIM36 affected ferroptosis in PCa, we detected the ferroptosis-related genes Recombinant Solute Carrier Family 7, Member 11 (Slc7a11), Peroxiredoxin 6 (Prdx6), and GPx4 protein expression, we found that the expression of GPx4 was negatively correlated with TRIM36 expression, while Slc7a11 and Prdx6 were not related to TRIM36 protein expression (Figure S3). At the same time, Western blotting results showed the expression of GPx4 was positively correlated with HK2 expression, which was negatively regulated by TRIM36 in PCa cells (Figure 6A). To further verify our results, we detected the GPx4 expression in PCa cells which were treated with HK2 inhibitor 3BP. The results showed that the expression of GPx4 decreased with HK2 inhibition (Figure 6B). These conclusions indicate that HK2 regulated the expression of GPX4 and the NED of PCa at the same time. We assumed that HK2 affected the NED of PCa by regulating GPX4. We tested the NED-related indicators in PCa cells treated with GPx4 inhibitor (1S,3R)-RSL3 (rsl3). It was found that both GPx4 and NED-related indicator expression were inhibited by rsl3 in PCa cells (Figure 6C). At the same time, we also knocked down HK2 again based on the knockdown/overexpression of TRIM36 to verify our previous conclusions. The results showed that after the knockdown of HK2, the protein expression of NED markers of LNCaP-NC, LNCaP-ST, PC3-NC, and PC3-OV were reduced and GPX4 was inhibited (Figure 6D). Prostate cancer cell lines showed lower NED characteristics. This is consistent with the conclusions of the above in vitro cell experiments. To further evaluate our conclusions in vivo, we performed a xenotransplantation experiment in nude mice. TRIM36 knockdown promoted the growth of xenografts in mice while TRIM36 overexpression greatly inhibited their growth (Figure 6E,F). We used immunohistochemical analysis to detect the effects of TRIM36 expression on HK2, GPx4, and NED-related genes of PCa xenografts. The results in the xenografts were consisted with the conclusion of the PCa cell experiments (Figure 6G). Our research revealed that TRIM36 inhibited the NED of PCa by inhibiting the expression of the key glycolytic enzyme HK2 and ferroptosis-related genes GPx4 (Figure 6H).

4 | DISCUSSION

Recent studies have shown that TRIM36 is essential for carcinogenesis and tumor growth. Our previous experimental results have confirmed that TRIM36 can inhibit the invasion and proliferation of PCa.[14] According to our research results, Kimura et al. found that TRIM36 can enhance the tumor-suppressive effect by regulating the apoptosis-related pathway in PCa.[10] Here, we for the first time report that TRIM36 plays a critical role in NEPC.

Surgery or radiotherapy can result in a good prognosis for localized PCa, while metastatic PCa easily develops resistance against ADT and deteriorates into CRPC.[18] To inhibit CRPC, the high-affinity AR receptor antagonist can achieve good outcomes, but may increase the risk of NEPC.[19,20] Our previous studies found that in the treatment of PCa, Ar receptor antagonists can inhibit TRIM36 expression[14] and accelerate the NED of the PCa cell line.[21,22] We therefore evaluated the effect of TRIM36 on the NED of PCa, discovering that the expression of TRIM36 was negatively correlated with NED biogenesis-related factor levels, according to TCGA database. Interestingly, TCGA database analysis revealed that the Gleason score (Gleason grading is a widely used histological grading method for prostate adenocarcinoma, a higher Gleason score indicates a stronger malignancy of prostate cancer) of PCa increased as TRIM36 expression decreased. As a highly invasive subtype of PCa, NEPC does not secrete prostate-specific antigen. Morphologically, NEPC shares some characteristics with small-cell carcinoma and does not express AR, but positively expressing NED-markers such as ENO2, AURKA, and SYP.[23] We verified the negative correlation between the expression of TRIM36 and NEPC markers (ENO2, AURKA, and SYP) in vivo and in vitro by construction of prostate cancer cell lines with knockdown and overexpression of TRIM36. The results were further confirmed in primary PCa and NEPC samples. Together, TRIM36, as a novel androgen-responsive gene, plays a critical role in NEPC and may serve as a therapeutic marker.

During glycolysis, glucose, on anoxic exposure, is converted into pyruvate, then into lactic acid. However, despite high oxygen in tumor cells, glycolysis is still active enough to produce a large amount of lactic acid, a phenomenon that is called the Warburg

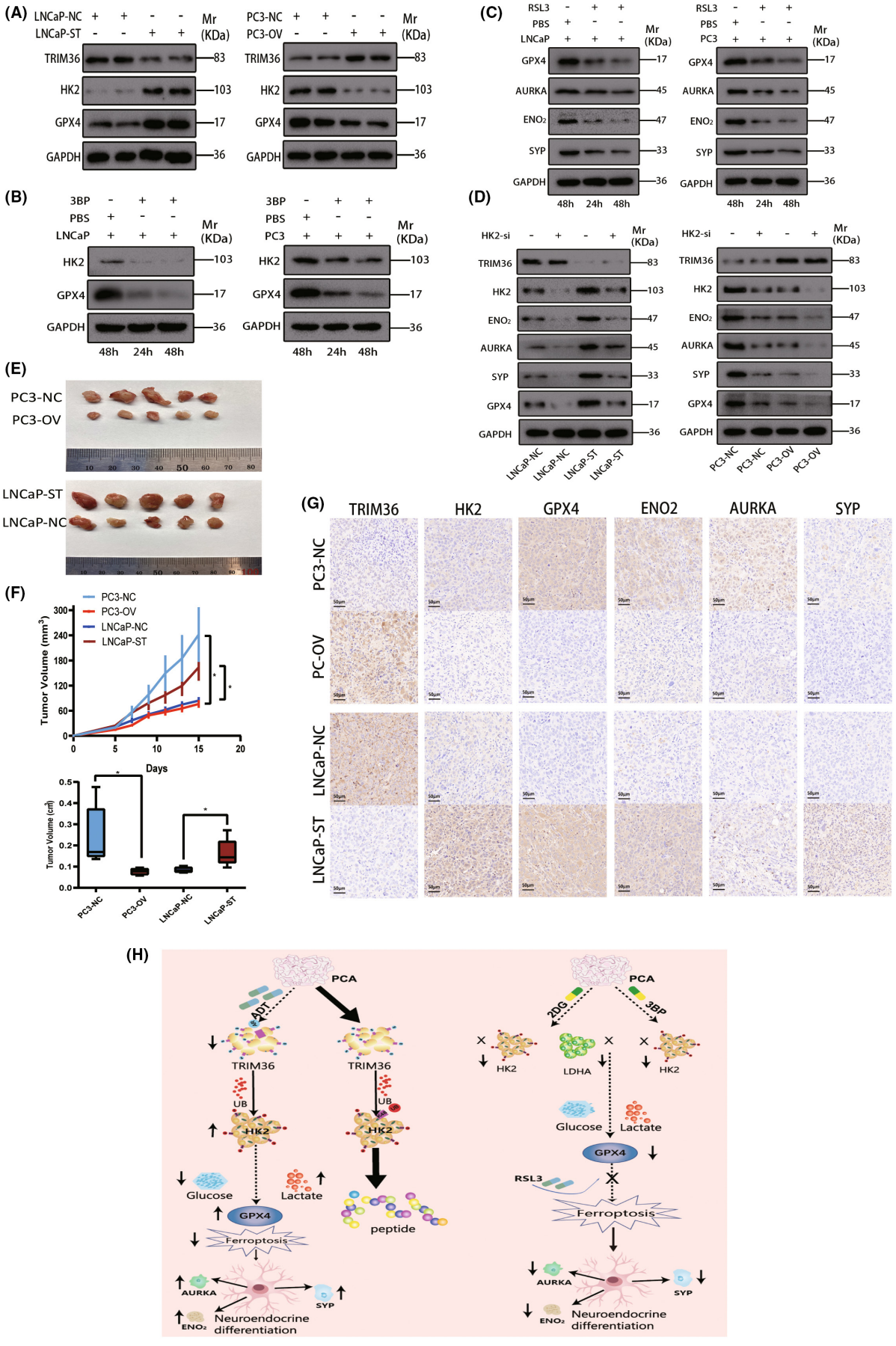
(A)
LNCaP-NC
LNCaP-ST
PC3-NC
PC3-OV
Mr (KDa)
TRIM36
HK2
GPX4
GAPDH
83
103
17
36
(B)
3BP
PBS
LNCaP
PC3
48h 24h 48h
(C)
RSL3
AURKA
ENO2
SYP
45
47
33
(D)
HK2-si
(E)
PC3-NC
PC3-OV
LNCaP-ST
LNCaP-NC
(F)
Tumor Volume (mm3)
Days
Tumor Volume (cm3)
(G)
TRIM36
HK2
GPX4
ENO2
AURKA
SYP
(H)
PCA
ADT
2DG
3BP
UB
peptide
Glucose
Lactate
LDHA
Ferroptosis
Neuroendocrine differentiation

FIGURE 6 TRIM36 regulated NED of PCa cells via HK2-GPX4-ferroptosis and inhibited the NED of PCa xenografts by inhibiting the expression of HK2 and GPx4. (A) The protein expression levels of glycolysis-related genes HK2 and ferroptosis-related genes GPx4 in LNCaP-ST, PC3-OV, and control cells. (B) Western blotting was used to detect the expression of glycolysis-related genes HK2 and ferroptosis-related genes GPx4 in PCa cells before and after 3BP treatment. (C) The expression of ferroptosis-related genes GPx4 and NED-related genes in PCa cells before and after RSL3 treatment was detected by Western blotting. (D) Western blotting to detect the protein expression of ferroptosis-related genes GPx4 and NED-related genes after hk2 knockdown in PCa cells. (E) LNCaP-NC, LNCaP-ST, PC3-NC, and PC3-OV cells were injected subcutaneously into the right abdomen of nude mice. Two weeks after cell injection, the tumor was harvested as shown. (F) Nude mouse xenograft tumor growth curve and volume plot. These values are expressed as mean ± SEM ($n = 5$). $^{*}P < 0.05$, $^{**}P < 0.01$. (G) Representative immunohistochemical stains of HK2, ENO_2, AURKA, and SYP from tumor xenografts in nude mice. Scale bar: 50 μm. (H) TRIM36 promotes the occurrence of ferroptosis and finally inhibits the NED of PCA cells by inhibiting the ferroptosis-related gene GPX4 through HK2 in the ubiquitin glycolysis pathway. The treatment of PCa by ADT induced the decrease in AR, which led to the decrease in the AR-response gene TRIM36. The decrease in TRIM36 expression inhibited HK2 ubiquitination and reduced the degradation of HK2. Increased HK2 expression activated the glycolysis pathway of PCa, promoted the expression of GPX4, inhibited ferroptosis, and ultimately led to the NED of PCa. Treating PCa cells with glycolysis inhibitor 2DG or HK2 inhibitor 3BP can effectively inhibit the glycolysis of PCa, thus inhibiting the expression of GPX4, promoting the occurrence of ferroptosis, and ultimately inhibiting the NED of PCa.

effect.[24] By inhibiting the Warburg effect and blocking the energy supply in tumor cells, tumor progression can be effectively inhibited. However, unlike in other malignant tumors, glycolysis mainly acts in the late stage of PCa.[25,26] Immunohistochemical staining has shown that lactate production and glycolysis are upregulated in NEPC, an end stage of advanced PCa.[27] This suggests that the NED of PCa is closely related to glycolysis. However, few studies have been carried out to discover the underlying mechanism. In our study, the mass spectrometry-based quantitative proteomics studies, including KEGG pathway analysis, were performed to explore TRIM36-induced potential pathogenesis in NEPC. We identified the differentially expressed proteins based on TRIM36-changed PCa cells, and the differentially expressed proteins mainly enriched in the glycolysis pathway. In vitro, glycolysis assay uncovered that TRIM36 inhibited the NED of PCa through the glycolysis pathway. Furthermore, as the key glycolytic enzyme, HK2 showed a significantly different expression compared with other glycolysis-related proteins. Interestingly, the significantly negative correlation between TRIM36 and HK2 expression was only observed at the protein level and TRIM36 is an E3-ubiquitinated ligase,[28,29] therefore we evaluated the ubiquitination level of HK2 in PCa cell lines. The IP experiment confirmed that TRIM36 specifically binds to HK2 at the protein level, and the change in TRIM36 affects the ubiquitination level of HK2. At the same time, the treatment of cells with MG132 proved that TRIM36 can promote its degradation through ubiquitination of HK2. We also found that the K48R ubiquitin mutant impaired HK2 polyubiquitation and K48 linked ubiquitin protein changes with TRIM36 expression. Our results confirm that TRIM36 can specifically bind to lys48 to mediate the ubiquitination of HK2 and reduce its protein expression, thus inhibiting the NED of PCa.

Recent insights indicate that ferroptosis is intrinsically linked with multiple cellular metabolic pathways, including energy, lipid, and amino acid metabolism, which directly affects the cell's susceptibility to lipid peroxidation and ferroptosis.[30–32] The glucose metabolism in malignant tumor cells is usually rewired to glycolysis to meet their increasing demands for energy and biosynthetic precursors, as well as maintenance of redox homeostasis to prevent ferroptosis. For instance, it has been observed that tumor cells undergo a high level of glycolysis to compensate for their intrinsically low ATP-generating efficiency.[33,34] Meanwhile, the inhibition of ferroptosis induced by glycolysis is not permanent and can be reversed when glycolysis is inhibited.[35] Interestingly, we found that TRIM36 could indirectly affect the activity of its ferroptosis-regulating gene GPx4 by affecting the expression of the key glycolytic enzyme HK2 in prostate cancer cells, and the expression of GPx4 decreased when treated with HK2 inhibitor 3BP. To further explore the relationship between ferroptosis and NED of PCa, we treated prostate cancer cells LNCaP and PC3 with GPx4 inhibitor rsl3 and found that the expression of NED indexes AURKA, ENO2, and SYP decreased, suggesting that ferroptosis may be closely related to NED of PCa. Finally, with the HK2 knockdown experiment, we got the same conclusions as the above experiments. The decrease in HK2 inhibited GPX4, resulting in decreased protein expression of NED markers in PCa cell lines. However, the internal mechanism is still unclear and needs to be further explored. Finally, we obtained the same results in xenotransplantation experiments in nude mice, which demonstrated in vivo that the metabolic regulation of TRIM36 can affect the NED of PCa. All these provided new ideas for the study of NEPC treatment.

In conclusion, TRIM36 can regulate the glycolysis metabolic pathways of PCa, sensitize PCa to ferroptosis, and ultimately lead to the inhibition of NEPC. This mechanism has great potential to design new strategies to retard NED and treat NEPC.

AUTHOR CONTRIBUTIONS

X.Z. performed the research, interpreted the data, and wrote the manuscript. X.Z., T.Z., Y.W., C.N., L.D., and S.S. performed the research. M.B., H.D., and C.L. provided material and skills and assisted in establishing techniques. J.L. and C.L. designed the experiment, and critically reviewed and approved the manuscript.

ACKNOWLEDGEMENTS

This study was supported by the National Natural Science Foundation of China (Grant no. 82002718), the Jiangsu Natural Science Foundation (Grant no. BK20191077), and Jiangsu Provincial

People's Hospital Clinical Capacity Enhancement Project (No. JSPH-MC-2021-12).

CONFLICT OF INTEREST STATEMENT

The authors have no conflict of interest.

ETHICS STATEMENT

I state that the protocol for the research project has been approved by a suitably constituted Ethics Committee of the institution within which the work was undertaken and that it conforms to the provisions of the Declaration of Helsinki.

Approval of the research protocol by an Institutional Reviewer Board. N/A.

Informed Consent. N/A.

Registry and the Registration No. of the study/trial. N/A.

Animal Studies. N/A.

ORCID

Chao Liang https://orcid.org/0000-0002-0598-0779

REFERENCES

1. Chang PC, Wang TY, Chang YT, et al. Autophagy pathway is required for IL-6 induced neuroendocrine differentiation and chemoresistance of prostate cancer LNCaP cells. *PLoS One*. 2014;9(2):e88556.
2. Ismail AH, Landry F, Aprikian AG, Chevalier S. Androgen ablation promotes neuroendocrine cell differentiation in dog and human prostate. *Prostate*. 2002;51(2):117-125.
3. Ritch CR, Cookson MS. Advances in the management of castration resistant prostate cancer. *BMJ*. 2016;355:i4405.
4. Virgo KS, Basch E, Loblaw DA, et al. Second-line hormonal therapy for men with chemotherapy-naive, castration-resistant prostate cancer: American Society of Clinical Oncology provisional clinical opinion. *J Clin Oncol*. 2017;35(17):1952-1964.
5. Kahn B, Collazo J, Kyprianou N. Androgen receptor as a driver of therapeutic resistance in advanced prostate cancer. *Int J Biol Sci*. 2014;10(6):588-595.
6. Watson PA, Chen YF, Balbas MD, et al. Constitutively active androgen receptor splice variants expressed in castration-resistant prostate cancer require full-length androgen receptor. *Proc Natl Acad Sci U S A*. 2010;107(39):16759-16765.
7. Kitamura K, Tanaka H, Nishimune Y. Haprin, a novel haploid germ cell-specific RING finger protein involved in the acrosome reaction. *J Biol Chem*. 2003;278(45):44417-44423.
8. Balint I, Muller A, Nagy A, Kovacs G. Cloning and characterisation of the RBCC728/TRIM36 zinc-binding protein from the tumor suppressor gene region at chromosome 5q22.3. *Gene*. 2004;332:45-50.
9. Takayama K, Tsutsumi S, Katayama S, et al. Integration of cap analysis of gene expression and chromatin immunoprecipitation analysis on array reveals genome-wide androgen receptor signaling in prostate cancer cells. *Oncogene*. 2011;30(5):619-630.
10. Kimura N, Yamada Y, Takayama KI, et al. Androgen-responsive tripartite motif 36 enhances tumor-suppressive effect by regulating apoptosis-related pathway in prostate cancer. *Cancer Sci*. 2018;109(12):3840-3852.
11. Warburg O. On the origin of cancer cells. *Science*. 1956;123(3191):309-314.
12. Chen F, Chen J, Yang L, et al. Extracellular vesicle-packaged HIF-1alpha-stabilizing lncRNA from tumour-associated macrophages regulates aerobic glycolysis of breast cancer cells. *Nat Cell Biol*. 2019;21(4):498-510.
13. Lee H, Zandkarimi F, Zhang Y, et al. Energy-stress-mediated AMPK activation inhibits ferroptosis. *Nat Cell Biol*. 2020;22(2):225-234.
14. Liang C, Wang S, Qin C, et al. TRIM36, a novel androgen-responsive gene, enhances anti-androgen efficacy against prostate cancer by inhibiting MAPK/ERK signaling pathways. *Cell Death Dis*. 2018;9(2):155.
15. Beltran H, Prandi D, Mosquera JM, et al. Divergent clonal evolution of castration-resistant neuroendocrine prostate cancer. *Nat Med*. 2016;22(3):298-305.
16. Kirkin V, McEwan DG, Novak I, Dikic I. A role for ubiquitin in selective autophagy. *Mol Cell*. 2009;34(3):259-269.
17. Pankiv S, Clausen TH, Lamark T, et al. p62/SQSTM1 binds directly to Atg8/LC3 to facilitate degradation of ubiquitinated protein aggregates by autophagy. *J Biol Chem*. 2007;282(33):24131-24145.
18. Miller KD, Siegel RL, Lin CC, et al. Cancer treatment and survivorship statistics, 2016. *CA Cancer J Clin*. 2016;66(4):271-289.
19. Beltran H, Tagawa ST, Park K, et al. Challenges in recognizing treatment-related neuroendocrine prostate cancer. *J Clin Oncol*. 2012;30(36):e386-e389.
20. Hirano D, Okada Y, Minei S, Takimoto Y, Nemoto N. Neuroendocrine differentiation in hormone refractory prostate cancer following androgen deprivation therapy. *Eur Urol*. 2004;45(5):586-592.
21. Santoni M, Conti A, Burattini L, et al. Neuroendocrine differentiation in prostate cancer: novel morphological insights and future therapeutic perspectives. *Biochim Biophys Acta*. 2014;1846(2):630-637.
22. Yuan TC, Veeramani S, Lin FF, et al. Androgen deprivation induces human prostate epithelial neuroendocrine differentiation of androgen-sensitive LNCaP cells. *Endocr Relat Cancer*. 2006;13(1):151-167.
23. Sargos P, Ferretti L, Gross-Goupil M, et al. Characterization of prostate neuroendocrine cancers and therapeutic management: a literature review. *Prostate Cancer Prostatic Dis*. 2014;17(3):220-226.
24. Hsu PP, Sabatini DM. Cancer cell metabolism: Warburg and beyond. *Cell*. 2008;134(5):703-707.
25. Oyama N, Akino H, Suzuki Y, et al. The increased accumulation of [18F]fluorodeoxyglucose in untreated prostate cancer. *Jpn J Clin Oncol*. 1999;29(12):623-629.
26. Effert PJ, Bares R, Handt S, Wolff JM, Bull U, Jakse G. Metabolic imaging of untreated prostate cancer by positron emission tomography with 18fluorine-labeled deoxyglucose. *J Urol*. 1996;155(3):994-998.
27. Choi SYC, Ettinger SL, Lin D, et al. Targeting MCT4 to reduce lactic acid secretion and glycolysis for treatment of neuroendocrine prostate cancer. *Cancer Med*. 2018;7:3385-3392.
28. Reymond A, Meroni G, Fantozzi A, et al. The tripartite motif family identifies cell compartments. *EMBO J*. 2001;20(9):2140-2151.
29. Gushchina LV, Kwiatkowski TA, Bhattacharya S, Weisleder NL. Conserved structural and functional aspects of the tripartite motif gene family point towards therapeutic applications in multiple diseases. *Pharmacol Ther*. 2018;185:12-25.
30. Venkatesh D, O'Brien NA, Zandkarimi F, et al. MDM2 and MDMX promote ferroptosis by PPARalpha-mediated lipid remodeling. *Genes Dev*. 2020;34(7–8):526-543.
31. Conrad M, Kagan VE, Bayir H, et al. Regulation of lipid peroxidation and ferroptosis in diverse species. *Genes Dev*. 2018;32(9–10):602-619.
32. Badgley MA, Kremer DM, Maurer HC, et al. Cysteine depletion induces pancreatic tumor ferroptosis in mice. *Science*. 2020;368(6486):85-89.
33. Rajeshkumar NV, Dutta P, Yabuuchi S, et al. Therapeutic targeting of the Warburg effect in pancreatic cancer relies on an absence of p53 function. *Cancer Res*. 2015;75(16):3355-3364.

34. Chesney J, Mitchell R, Benigni F, et al. An inducible gene product for 6-phosphofructo-2-kinase with an AU-rich instability element: role in tumor cell glycolysis and the Warburg effect. *Proc Natl Acad Sci U S A*. 1999;96(6):3047-3052.
35. Marchiq I, Le Floch R, Roux D, Simon MP, Pouyssegur J. Genetic disruption of lactate/H+ symporters (MCTs) and their subunit CD147/BASIGIN sensitizes glycolytic tumor cells to phenformin. *Cancer Res*. 2015;75(1):171-180.

SUPPORTING INFORMATION

Additional supporting information can be found online in the Supporting Information section at the end of this article.

How to cite this article: Zhao X, Zhou T, Wang Y, et al. Trigred motif 36 regulates neuroendocrine differentiation of prostate cancer via HK2 ubiquitination and GPx4 deficiency. *Cancer Sci*. 2023;114:2445-2459. doi:10.1111/cas.15763